J Mater Sci: Mater Med (2015) 26:206
DOI 10.1007/s10856-015-5539-7

Original Research

The grafting of a thin layer of poly(sodium styrene sulfonate) onto poly(ε-caprolactone) surface can enhance fibroblast behavior

Géraldine Rohman[1] · Stéphane Huot[1] · Maria Vilas-Boas[1] · Gabriela Radu-Bostan[1] · David G. Castner[2] · Véronique Migonney[1]

Received: 12 January 2015 / Accepted: 3 July 2015 / Published online: 9 July 2015

Abstract Poly(sodium styrene sulfonate) (pNaSS) was grafted onto poly(ε-caprolatone) (PCL) surfaces via ozonation and graft polymerization. The effect of ozonation and polymerization time, as well as the Mohr's salt concentration in the grafting solution, on the degree of grafting was investigated. The degree of grafting was determined through toluidine blue staining. The surface chemical change was characterized by attenuated total reflection Fourier transform infrared spectroscopy, energy-dispersive X-ray spectroscopy and X-ray photoelectron spectroscopy. The result demonstrated that the grafting did not induce any degradation of PCL, and that pNaSS was grafted onto PCL as a thin and covalently stable layer. Furthermore, the modified PCL surface reveals a significant increase in the metabolic activity of fibroblastic cells, as well as a better cell spreading with higher adhesion strength. Consequently, bioactivity of PCL is greatly enhanced by immobilizing a thin layer of pNaSS onto its surface. The grafting of pNaSS is a promising approach to increase the bioactivity of PCL-based materials used in tissue engineering applications, such as ligament reconstruction.

✉ Géraldine Rohman
geraldine.rohman@univ-paris13.fr

[1] Université Paris 13, Sorbonne Paris Cité, Laboratoire de Chimie, Structures, Propriétés de Biomatériaux et d'Agents Thérapeutiques (CSPBAT), CNRS UMR 7244, 93430 Villetaneuse, France

[2] National ESCA and Surface Analysis Center for Biomedical Problems (NESAC/Bio), Departments of Bioengineering and Chemical Engineering, University of Washington, Box 351653, Seattle, WA, USA

1 Introduction

One of the major goals of tissue engineering is to develop biodegradable scaffolds that would allow cell adhesion, proliferation and differentiation in a three-dimensional structure. If the aspect of biodegradability generally motivates the choice of α-hydroxy polyesters as the scaffolding matrix: the major disadvantage of aliphatic polyesters is the absence of cell signaling promoting good cell response. To overcome the chemical composition problem encountered by polyester materials, a variety of approaches have been proposed to change the material surface: introduction of polar groups by surface treatment, adsorption of biomolecules, and covalent immobilization of bioactive compounds [1–5]. This last approach has the advantage to improve biocompatibility while incorporating some durability in comparison with adsorption methods in which biomolecules may desorb rapidly. However, there are many factors that influence how the biomolecule is tethered to the surface and, as a consequence, its bioactivity [1]. Moreover, when using biomolecules such as glycosaminoglycans, the understanding of the biomolecule influence on cell proliferation can be difficult because of its heterogeneity. In fact, dispersity of molecular weights, net charges and distribution of ionic groups can significantly influence the biological response [1, 3]. In addition, the cost and the control of biomolecule immobilization remain a critical step for controlling the cell response. Thus, the introduction of functional groups is an easier way to change the charge or the chemical composition surface of a substrate, and therefore to modulate the rearrangements of proteins that adsorb from the cell culture serum onto the substrate surface [6].

Modification of polyesters by graft copolymerization of anionic and hydrophilic monomers is a well-known

versatile method for enhancing the in vitro and in vivo cell behavior. Sulfated macromolecules or monomers have been widely used to design polymeric biomaterials with good blood compatibility and anticoagulation activity [7]. Interestingly, it was found that the grafting of poly(sodium styrene sulfonate) (pNaSS) onto poly(ethylene) substrates led to a high adhesion of HeLa S3 [8] and Chinese hamster ovary cells [9]. Kishida et al. [8] suggested that the presence of the aromatic ring close to the ionizable sulfonate group permitted high protein adsorption to the pNaSS surface. Recently, our group demonstrated that when pNaSS was grafted from poly(ethylene terephthalate) (PET)-based synthetic ligaments, pNaSS allowed a stronger fibroblast adhesion, a better cell spreading, a more homogeneous cell distribution over the material surface, and an increase in the cell collagen secretion [10, 11]. The same effect of pNaSS is observed when it is grafted from non-polymeric biomaterial surfaces [12–15]. Indeed, when pNaSS was grafted from titanium surfaces, the level of protein adsorption was increased and the adsorbed proteins were also modulated selectively compared to native titanium surfaces [12]. In addition, the adhesion of MG63 [13] or human mesenchymal stem cells [14] and their spreading were enhanced on the pNaSS grafted surfaces. Moreover, a better alkaline phosphatase ALP activity and mineralization were found on pNaSS grafted surfaces, underscoring the effect of pNaSS on the osteoblastic differentiation [14]. Finally, when PET-based synthetic ligaments were implanted in an ovine model for anterior cruciate ligament reconstruction, the pNaSS grafting enhanced direct ligament-to-bone contact with a decrease of fibrous scar tissue at the bone/ligament interface [11, 16]. Thus, the immobilization of pNaSS into three-dimensional scaffolds used in tissue engineering applications, especially in ligament reconstruction, may effectively modulate the cell response and seems to be a good alternative to the covalent immobilization of more complex biomolecules.

However, sodium styrene sulfonate (NaSS) is an anionic vinyl monomer which is known for its poor polymerization kinetics because of the incompatibility between highly ionized sulfonic acid groups surrounded by a large hydration spheres and hydrophobic polymer backbone [17]. Until now, pNaSS has not been covalently grafted onto biodegradable scaffolds based on synthetic polyesters such as poly(ε-caprolactone) (PCL), except from recent preliminary studies from our group [18, 19]. Indeed as PCL is a semi-crystalline biodegradable polymer with low characteristic temperatures (glass transition temperature around −60 °C and melting point temperature ranging between 59 and 64 °C [20, 21]), the grafting can only be carried out in mild conditions to avoid the degradation of PCL and drastic changes in thermal and mechanical properties. Thus, it is required to develop a versatile strategy that allows an effective grafting of pNaSS from PCL while maintaining the bioactivity of pNaSS and the intrinsic properties of PCL-based biomaterials.

In the present study, graft polymerization of NaSS onto PCL films was investigated under various reaction parameters: ozonation and polymerization time, as well as concentration of Mohr's salt in the grafting solution. The evidence of pNaSS grafting was demonstrated by wettability measurements, attenuated total reflection Fourier transform infrared spectroscopy (ATR-FTIR), energy-dispersive X-ray spectroscopy (EDX) and X-ray photoelectron spectroscopy (XPS). The degree of grafting was determined through toluidine blue staining. The effect of pNaSS grafting on fibroblast behavior was evaluated through in vitro assays that measure cell metabolic activity and morphology.

2 Materials and methods

2.1 Materials

PCL was obtained from Sigma-Aldrich. NaSS (Sigma-Aldrich) was purified by recrystallization in a distilled water/ethanol solution (10/90 % (v/v)). Mohr's salt, potassium iodide and toluidine blue (BT) (Sigma-Aldrich) were used without any purification. All solvents were purchased from Fisher and used as received. Phosphate buffered saline solution (PBS), Dulbecco's modified eagle medium (DMEM), penicillin–streptomycin (PenStrep), and foetal bovine serum (FBS) were supplied by Gibco. MTT (3-(4,5-dimethylthiazol-2-yl)-2,5-diphenyl tetrazolium salt), phalloidin-FITC and Hoechst 33258 were purchased from Sigma. McCoy fibroblasts were purchased from ATCC (CRL-1696, USA).

2.2 Preparation of PCL films and grafting of pNaSS

The films were manufactured using a spin-coating method. A PCL solution in dichloromethane (60 % (w/v)) was dropped onto a glass slide and then spun for 30 s at 1500 rpm using a SPIN150-v3 SPS. The films were air-dried for 2 h and then vacuum-dried for 24 h to remove the solvent, and finally they were cut into small disks with a diameter of ∼15.5 mm.

For the pNaSS grafting, the films were suspended under stirring into distilled water at room temperature. Ozone was generated using an ozone generator BMT 802 N (ACW) with a pressure of 0.5 bar and an oxygen flow rate of 0.6 L min^{-1}. After ozonation, the PCL films were transferred into a degassed NaSS solution in distilled water (15 % (w/v)) containing Mohr's salt. The system was maintained at 45 °C to allow the graft polymerization to

occur. After polymerization, the samples were washed with distilled water overnight and finally vacuum-dried.

The films were sterilized and prepared by successive immersions as follows: 2 h in 70 % ethanol, 2 h in sterile PBS solution, 1 h in DMEM, and 1 h in complete medium.

2.3 Quantitative determination of peroxide generated from ozonation and pNaSS grafted after polymerization

The amount of peroxide generated by the ozonation in the PCL films was determined by a spectrophotometric method (iodide method) [22]. Two films were placed in 1 mL of isopropanol and 7 mL of a potassium iodide solution containing 1 ppm-ferric chloride, and kept at 45 °C for 10 min. After the reaction, the oxidized iodine was immediately measured by following the triiodide anion concentration by using a spectrophotometer (Perkin Elmer Lambda 25) to measure the absorbance of the solution at 360 nm. The method was calibrated through the use of benzoyl peroxide. The density of peroxide was expressed in mol of peroxide per cm^2 of PCL film.

The amount of pNaSS grafted onto PCL films was determined by a colorimetric method through the complexation of BT with the sulfonate groups of pNaSS. Briefly, one film was placed in 5 mL of BT solution and kept at 30 °C for 6 h. After the reaction, the complexed BT was decomplexed in 10 mL of acetic acid solution (50 % (v)) for 24 h at room temperature. Thereafter, the absorbance of the solution was measured at 633 nm using a spectrophotometer (Perkin Elmer Lambda 25). The method was calibrated through the use of BT solutions in acetic acid. The grafting density (GD) was expressed in mol of pNaSS per cm^2 of PCL film.

2.4 PCL characterization

The PCL number-average and weight-average molecular weights (Mn and Mw, respectively) and the polydispersity index (PDI) were determined using size exclusion chromatography (SEC) using a Spectra Physics P100 pump equipped with a refractive index detector (Wyatt Technology Optilab Rex). Two samples were analyzed for each film condition. The samples were dissolved in tetrahydrofuran and eluted through 2 mixed C-13 columns (Polymer Laboratories) connected in series at a flow rate of 1 mL min^{-1}. The sample concentration was 10 mg mL^{-1} and a conventional calibration was generated with a series of narrow polydispersity polystyrene standards.

Differential scanning calorimetry (DSC) analyses were carried out with a 131 Seratam Instrumentation calorimeter under a nitrogen atmosphere. Two samples were analyzed for each film condition. Samples were scanned one time from 25 to 200 °C at a heating rate of 10 °C min^{-1}. The melting temperature (T_m) and the melting enthalpy (ΔH_m) of PCL were determined from the first scan; the melting temperature was taken at the maximum of the peak. Thereafter, the samples were scanned twice from -100 to 25 °C at a heating rate of 10 °C min^{-1}. The glass transition temperature (T_g) was determined at the mid-point from the second scan. The degree of crystallinity (Xc) was calculated using Eq. 1:

$$\mathrm{Xc}\,(\%) = \frac{\Delta H_m}{\Delta H_m^0} \times 100 \quad (1)$$

where ΔH_m^0 stands for the melting enthalpy of 100 % crystalline PCL ($\Delta H_m^0 = 135$ J g^{-1}) [23].

2.5 Surface analyses

Contact angle (θ) measurements were performed by the sessile drop method using Drop Shape Analysis software and a KRUSS equipment. The liquid utilized was distilled water, and 3 measurements were done for each sample at different positions. Two samples were analyzed for each film condition.

Fourier-transformed infrared (FTIR) spectra, recorded in an attenuated total reflectance mode (ATR), were obtained using a SMART OMNIC-sampler connected to a Thermo Nicolet Avatar 6700 FTIR and controlled by OMNIC software. The spectra were obtained by accumulating 128 scans in the range 650–4000 cm^{-1} with a resolution of 4 cm^{-1}. Background scans were acquired without the sample present.

Energy-dispersive X-ray spectroscopy (EDX) analyses were performed using an environmental scanning electron microscope (ESEM—Hitachi TM3000) operating at an accelerated voltage of 15 kV and equipped with an EDX probe (Hitachi SwiftED3000). The acquisition time was set to 196.6 s. Three samples were analyzed for each film condition.

X-ray photoelectron spectroscopy (XPS) analyses were performed using a Surface Science Instruments S-probe spectrometer. This instrument has a monochromatized Al Kα X-ray and a low energy electron flood gun for charge neutralization of non-conducting samples. The take-off angle was 55°. Service Physics Hawk Data Analysis 7 Software was used to calculate surface atomic concentrations from peak areas taken from the survey and detail scans and then corrected with the appropriate elemental sensitivity factors, as well as to peak fit the high resolution scans. The binding energy scales of the high-resolution spectra were calibrated by assigning the lowest binding energy C1 s high-resolution peak a binding energy of

285.0 eV. For compositional analysis, three different spots were analyzed from each sample type. A high resolution C1 s scan was acquired from one spot per sample.

2.6 Grafting stability

To study the stability of the pNaSS grafting, the sterilized films were immersed in sterile PBS (pH 7.1) and incubated at 37 °C in a humidified atmosphere of 5 % CO_2 in air for different periods of time. At the end of the incubation, the pH of PBS was monitored and the samples were washed in PBS overnight. The amount of grafted pNaSS remaining on incubated film was determined by the BT method and was calculated according to Eq. 2:

$$\text{Remaining pNaSS}\,(\%) = \frac{GD_t}{GD_i} \times 100 \qquad (2)$$

where GD_i and GD_t stand for the grafting density before incubation and after the incubation time t, respectively.

2.7 In vitro assays

After sterilization, the films were placed in individual wells of a 24-well plate and weighed down with a PTFE ring. McCoy cells were seeded onto the films at a cell density of 50,000 cells/well for 2 h at 37 °C. Subsequently, the wells were flooded above the PTFE ring with DMEM supplemented with PenStrep (1 %) and FBS (10 %). The cellular mitochondrial activity was measured after 24 h of culture though a modified MTT assay [24]. MTT solution in PBS (5 mg mL^{-1}) was added to each well and then incubated for 4 h at 37 °C. After that period of incubation, films were removed carefully and transferred into glass vials containing 500 µL of dichloromethane. After total dissolution of the films, 500 µL of dimethyl sulfoxide were added and samples were left overnight under agitation. The optical density was measure at 550 nm using a spectrophotometer (Perkin Elmer Lambda 25). Films maintained in culture without cells and analysed as above were used for background subtraction. The films were tested in triplicate. For a control, McCoy cells were seeded on commercial treated polystyrene culture dishes (TCPS).

For the morphology study, all images were taken after 48 h of culture. ESEM images were carried out using a Hitachi TM3000 ESEM operating at 15 kV and equipped with a Peltier stage operating at 4 °C. For this experiment, the cell density was 10,000 cells/well. For the fluorescent images, the samples were stained with Hoechst and/or phalloïdin and visualized with a fluorescence microscope (AXIOLAB HBO-500, ZEISS). Images were captured with PROGSPOT software. The cell density was 1000 cells/well or 50,000 cells/well.

2.8 Statistical analysis

Statistical analysis was performed using the Statistical Package for the Social Sciences (SPSS) software. For every population, group normality was checked by a Kolmogorov–Smirnov's test. The homogeneity of variances between the groups was assessed by a Levene's test and one-way ANOVA was performed for the inspection of statistical differences between the means. Finally, Tukey's and Scheffe's post hoc tests were carried out. In all statistical evaluations, $P < 0.05$ was considered as statistically significant.

3 Results

3.1 Grafting of pNaSS onto PCL films

The quantity of (hydro)peroxide generated in the PCL films during the ozonation, as determined by the iodide method, reached its highest value at 60 min ($(2.5 \pm 0.2) \times 10^{-8}$ mol cm^{-2}) (Fig. 1a). Longer ozonation times did not produce higher peroxide levels in PCL.

The grafting was first carried out for 3 h without Mohr's salt in the grafting solution. Similar to the peroxide results, the quantity of pNaSS grafted from the PCL films, as determined by the BT method, reached its highest value at 60 min ($GD = (3.6 \pm 0.9) \times 10^{-8}$ mol cm^{-2}) (Fig. 1a). Longer ozonation times did not lead to an increase in the concentration of grafted pNaSS. When the ozonation time was limited to 20 min and the Mohr's salt was introduced in the grafting solution, the grafting density increased as the concentration of Mohr's salt increased up to 2.5 % (w/v) (Fig. 1b). For salt concentrations above 2.5 % (w/v), the quantity of grafted pNaSS decreased. Increasing the polymerization time increased the grafting density, and the concentration of grafted pNaSS reached its highest value and a plateau after 6 h ($GD = (6.5 \pm 0.6) \times 10^{-8}$ mol cm^{-2}) (Fig. 1c). Longer polymerization time did not lead to an increase in the concentration of grafted pNaSS.

The stability of the grafted layer of pNaSS was studied by quantifying the amount of pNaSS remaining on the PCL films after incubation in PBS (pH 7.1) at 37 °C. As determined by the BT method, no loss of pNaSS was detected after 1 month of incubation (Fig. 2). Also, no significant variation of PBS pH was noticed.

3.2 PCL film properties

The PCL films were prepared with a diameter of 15.5 ± 0.2 mm and a thickness of 45 ± 5 µm. No variation in film dimensions was detected after the grafting of pNaSS. Table 1 summarizes the properties of the films

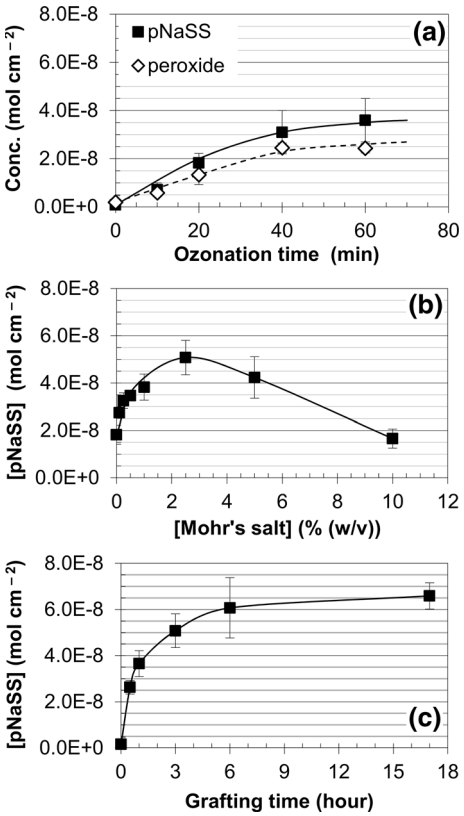

Fig. 1 Concentration of peroxide (*open diamond*) or grafted pNaSS (*filled square*) on PCL films as a function of various parameters: **a** effect of the ozonation time [grafting time = 3 h, (Mohr's salt) = 0 % (w/v)]; **b** effect of the Mohr's salt concentration in the grafting solution (process parameters: ozonation time = 20 min, grafting time = 3 h); **c** effect of the grafting time [process parameters: ozonation time = 20 min, (Mohr's salt) = 2.5 % (w/v)]

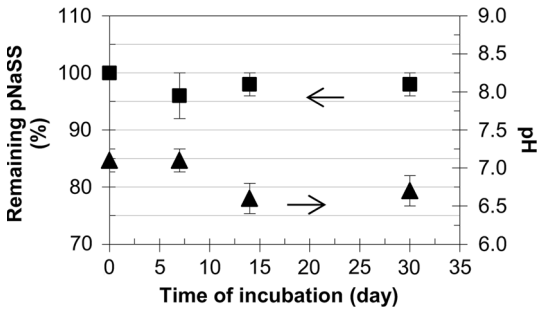

Fig. 2 Remaining pNaSS (square symbols) and PBS pH (triangular symbols) during 1 months of incubation of PCL films grafted with pNaSS (GD = (5.1 ± 0.7) × 10^{-8} mol cm^{-2}) in PBS (pH 7.1) at 37 °C

before and after grafting. The ungrafted PCL films have a number-average molecular weight of 25,400 g mol^{-1} and a polydispersity index of 1.6. The glass transition temperature was −63 ± 1 °C and the melting temperature was found to be 61 ± 1 °C with a crystallinity degree of 52 %. No significant variations in molecular weight, characteristic temperatures or degree of crystallinity occurred after pNaSS grafting.

3.3 Surface analysis

In addition to quantitative determination of pNaSS, the BT method revealed that the grafting was homogeneous across the film surface, as the blue coloration of the film before BT decomplexation was uniform. It was also found that the surface wettability had been modified after grafting as the water contact angle of the films decreased from 74 ± 3° for ungrafted PCL to 60 ± 5° for pNaSS grafted PCL.

Evidence for successful grafting of pNaSS was also obtained with infrared spectroscopy (Fig. 3). Several peaks that can be attributed to pNaSS in the spectrum of the grafted PCL film were observed: 1136 and 1011 cm^{-1} for the in-plane skeleton vibration and in-plane bending vibration of benzene ring, respectively; and 844 cm^{-1} for the deformation vibration of the C-H bond in the benzene

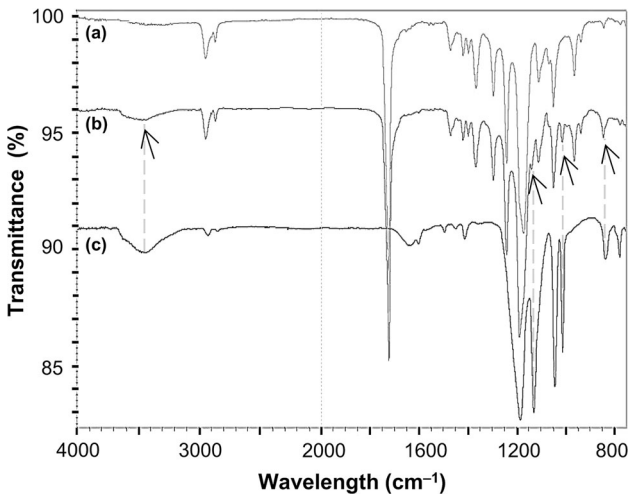

Fig. 3 ATR-FTIR analyses of: *a* PCL film before pNaSS grafting; *b* PCL film after pNaSS grafting (GD = (5.1 ± 0.7) × 10^{-8} mol cm^{-2}); *c* pNaSS

Table 1 Characteristics of ungrafted PCL films and PCL films grafted with pNaSS (GD = (5.1 ± 0.7) × 10^{-8} mol cm^{-2})

Sample	Mn (g mol^{-1})	PDI	T_g (°C)	T_m (°C)	Xc (%)
Ungrafted PCL films	25,400	1.6	−63 ± 1.0	61 ± 1.0	52
Grafted PCL films	23,400	1.6	−62 ± 1.0	62 ± 1.5	50

Mn molecular weight, *PDI* polydispersity index, T_g glass transition temperature, T_m melting temperature, *Xc* crystallinity degree

Table 2 EDX and XPS-determined surface elemental compositions of ungrafted PCL films and PCL films grafted with pNaSS (GD = (5.1 ± 0.7) × 10^{-8} mol cm^{-2})

Sample	Carbon	Oxygen	Sulfur	Sodium	Other
PCL (theory)	75.0	25.0	–	–	–
NaSS (theory)	61.5	23.1	7.7	7.7	–
EDX (at. %)					
Ungrafted PCL films	75.5 ± 0.3	24.5 ± 0.3	–	–	–
Grafted PCL films	73.4 ± 0.4	26.4 ± 0.4	0.15 ± 0.07	0.04 ± 0.04	Fe
XPS (at. %)					
Ungrafted PCL films	76.4 ± 1.7	22.4 ± 0.5	–	–	Si, F
Grafted PCL films	70.8 ± 1.9	24.1 ± 0.9	1.8 ± 0.6	0.8 ± 0.2	Si, Fe, F, N

The expected elemental compositions based on the stoichiometry of PCL and NaSS are included for comparison. Values are reported as averages and standard deviations. The atomic percent of other elements present in each type of sample is listed in decreasing order

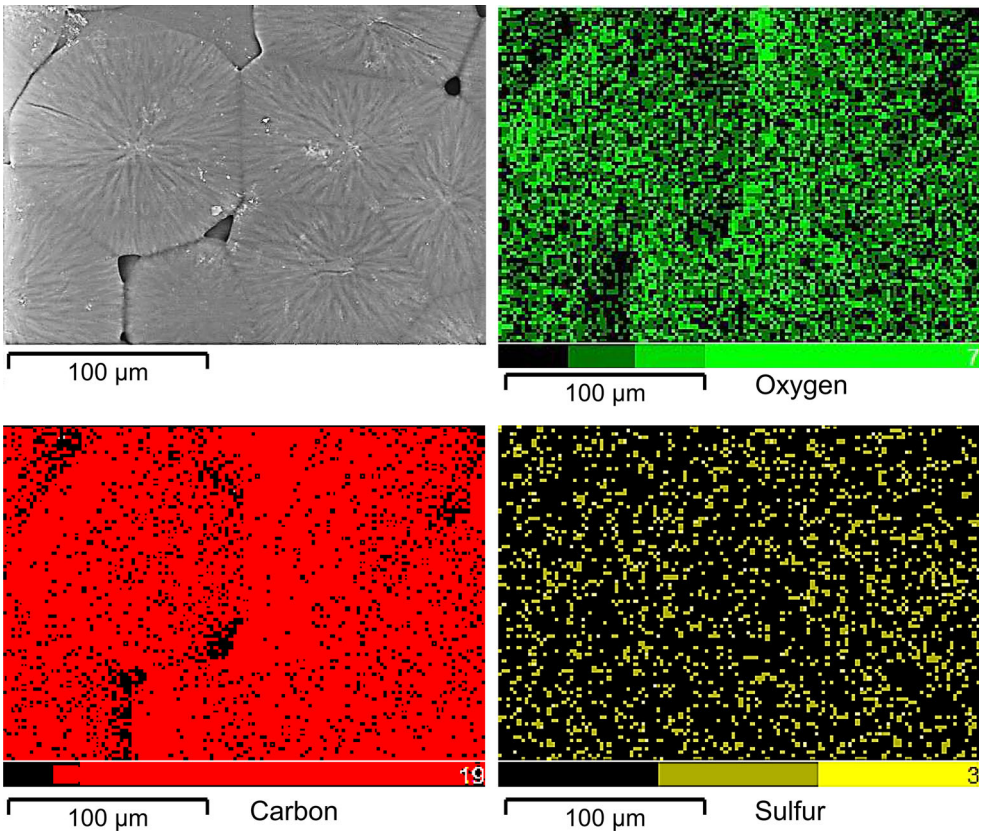

Fig. 4 EDX elemental mapping of PCL films after pNaSS grafting (GD = (5.1 ± 0.7) × 10^{-8} mol cm^{-2}) (accelerating voltage = 15 kV, acquisition time = 196.6 s)

ring. Finally, a small, broad peak appeared around 3430 cm^{-1} for the O–H stretching vibration of H_2O that interacts with pNaSS [25].

EDX and XPS analyses also confirmed the presence of pNaSS through the detection of sulfur and sodium atoms with a measured atomic content of 0.15 ± 0.07 and 0.04 ± 0.04 at. %, respectively for EDX analyses, and 1.8 ± 0.6 and 0.8 ± 0.2 at. %, respectively for XPS analyses (Table 2). The elemental mapping obtained by EDX confirmed the homogeneous distribution of the sulfonate groups over the PCL surface (Fig. 4).

The Na/S ratio obtained from EDX and XPS were significantly below the expected value of 1 from the NaSS structure, which indicates that sodium was removed during the final rinsing of the grafted samples. Small amounts of silicon (1.1 ± 1.6 at. %) and trace amounts of fluorine

(0.2 ± 0.3 at. %) were detected by XPS on the ungrafted PCL surfaces. Small amounts of silicon (2.2 ± 0.6 at. %), trace amounts of iron (0.2 ± 0.2 at. %), fluorine (0.1 ± 0.2 at. %) and nitrogen (0.1 ± 0.3 at. %) were detected on the grafted PCL surfaces. The presence of iron is likely due to the use of Mohr's salt in the grafting process.

The XPS high-resolution C1 s peak fitting of the PCL surfaces before and after pNaSS grafting, as well as the expected amounts of each carbon species based on the stoichiometry of NaSS, are shown in Table 3. It has to be noted that the C–O species of PCL overlap with the C–SO_3 species expected from NaSS. However for the grafted surfaces, the percentage of hydrocarbon species increased slightly, while the percentage of carboxylate ester species decreased slightly.

3.4 In vitro assays

McCoy cells were seeded over ungrafted and grafted PCL films, as well as TCPS for control. To evaluate the metabolic activity of cells, a MTT assay was carried out after 24 h of incubation on the surfaces (Fig. 5). A Kolmogorov–Smirnov's test ($P > 0.05$) showed that the data were approximately normally distributed for each samples. A Levene's test verified the homogeneity of variances in the samples ($P = 0.39$). A one-way ANOVA test showed that there was a statistically significant difference between the 3 samples ($P = 0.00$). A Tukey's post hoc test demonstrated that there was no statistically significant difference between the films grafted with pNaSS (% viability = 87.1 ± 6.5 %) and TCPS (% viability = 100.0 ± 6.5 %) ($P = 0.36$). However, a Scheffe's post hoc test revealed that there were statistically significant differences between the ungrafted films (% viability = 41.9 ± 16.1 %) and TCPS (% viability = 100.0 ± 6.5 %) ($P = 0.00$), as well as between the ungrafted films and the grafted films ($P = 0.01$). These results demonstrated that there was a significant increase in metabolic activity of cells that have been cultured onto the pNaSS grafted PCL films in comparison with the ungrafted PCL films.

After 48 h of incubation, examination of the cell morphology revealed that the cells were well spread and organized on the pNaSS grafted PCL films (Fig. 6d–f) compared to ungrafted PCL films, where cells were predominantly round or shapeless and disorganized (Fig. 6a–c). Focal points are visible when the cells were incubated on the grafted films, which show that the pNaSS surface is favorable to cell adhesion and proliferation (Fig. 6f). Moreover, fewer cells were found on the ungrafted films in comparison with the grafted ones.

Table 3 XPS high-resolution C1 s peak fitting results for ungrafted PCL films and PCL films grafted with pNaSS (GD = (5.1 ± 0.7) × 10^{-8} mol cm^{-2})

Sample	C–C/C–H	C–O/C–SO_3	O–C=O
XPS C1s (%)			
PCL (theory)	66.7	16.7	16.7
Ungrafted PCL films	71	15	15
Grafted PCL films	74	15	12
NaSS (theory)	87.5	12.5	–

The expected XPS carbon species based on the stoichiometry of PCL and are included for comparison. Values are reported as averages and standard deviations

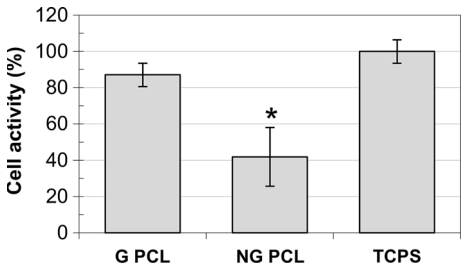

Fig. 5 Metabolic activity of McCoy fibroblasts after 24 h of culture onto the ungrafted PCL films (NG PCL), the PCL films grafted with pNaSS (G PCL/GD = (5.1 ± 0.7) × 10^{-8} mol cm^{-2}) in comparison with seeding onto commercial treated polystyrene culture dishes (TCPS) (*$P < 0.05$)

4 Discussion

The main goal of the study was to demonstrate the feasibility of bioactivating PCL through the grafting of NaSS without altering the PCL intrinsic properties. Kinetics of graft polymerization of NaSS from PCL films by preozonation method was investigated to determine the optimum reaction parameters. The effects of reaction parameters such as ozonation and polymerization time, as well as the concentration of Mohr's salt in the monomer solution, were established in correlation with the grafting density. Two-dimensional PCL films were prepared as model surfaces which do not undergo morphological variations after surface modification of the substrate, allowing a straightforward interpretation of cell response and an easy comparison with commercial treated polystyrene culture dishes.

4.1 Grafting of pNaSS onto PCL films

The first step of the process is the generation by ozonation of (hydro)peroxides over film surfaces. Indeed, the ozone oxidation of polymers leads to peroxy-radicals which then convert to various functionalities such as (hydro)peroxides,

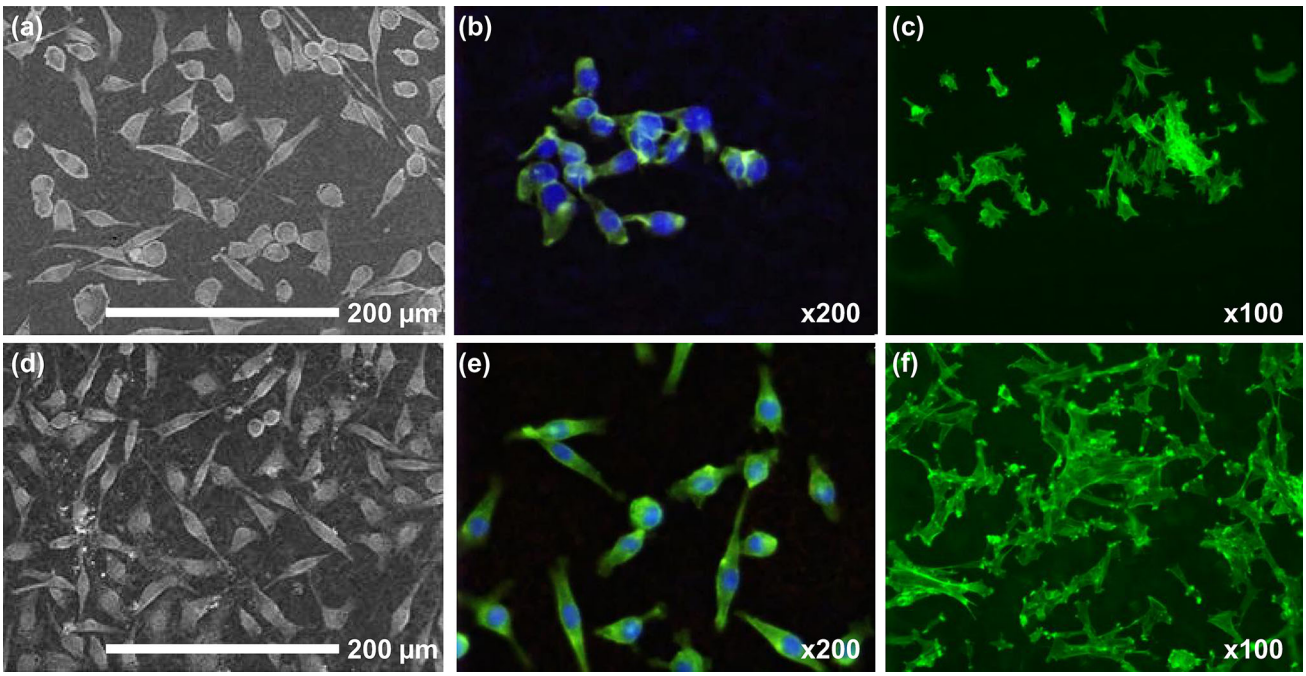

Fig. 6 Images of McCoy fibroblasts attached after 48 h of culture onto ungrafted PCL films (**a**, **b**, **c**) or PCL films grafted with pNaSS (GD = $(5.1 \pm 0.7) \times 10^{-8}$ mol cm^{-2}) (**d**, **e**, **f**). **a**, **d** ESEM images (cell seeding density = 10^4 cells per film); **b**, **e** fluorescent images with Hoechst 33258/Phalloidin-FITC staining (cell seeding density = 10^3 cells per film); **c**, **f** fluorescent images with Phalloidin-FITC staining (cell seeding density = 5×10^4 cells per film)

ketones, aldehydes, acids, etc. (Hydro)peroxides also react with ozone to convert-back to peroxy-radicals. Therefore with long ozonation times, the (hydro)peroxide concentration becomes constant and the other functionalities increase in concentration [26]. As expected, the peroxide concentration produced on the PCL films increased with the ozonation time and stabilized at a plateau for ozonation times longer than 60 min. The maximum value found for the PCL films is in good agreement with values found by Suh et al. for semi-crystalline poly(L-lactic acid) membranes ($(2.9 \pm 0.3) \times 10^{-8}$ mol cm^{-2}) [22].

The second step of the process is the covalent grafting by radical polymerization of NaSS at 45 °C. This temperature was selected as it is lower than the PCL melting temperature. However, even if the grafting of pNaSS was possible, the temperature is relatively low for the thermal peroxide decomposition and subsequent polymerization of NaSS [27]. To increase the grafting density, the polymerization was initiated through the redox decomposition of the peroxides by using Mohr's salt [27]. In addition, the use of Mohr's salt might prevent the side reaction of NaSS homopolymerization in solution. Indeed, it is well known that Fe^{2+} ferrous ions convert $HO^{\cdot}$ free radicals, generated in the solution by hydroperoxide decomposition, into HO^{-} inactive species. Nevertheless, high concentration of Fe^{2+} also leads to a decrease of the grafting density due to the deactivation of radicals present onto film surface [28, 29]. Furthermore, high concentration of Mohr's salt significantly increases the rate of peroxide decomposition, which will inhibit initiation of the graft polymerization [27]. The same trends were observed in this study with an increase of the grafting density up to 2.5 % (w/v) of Mohr's salt followed by a decrease. Longer polymerization time than 3 h did not lead to a significantly higher grafting density due to an increase of the homopolymerization of NaSS, as observed through an increase of the solution viscosity.

4.2 PCL film characterization

Polymer modification may affect various intrinsic material properties, such as the polymer molecular weight, the thermal properties and the crystallinity degree which as a consequence may lead to a wide variation in mechanical properties and degradation rates [30]. As expected, the pNaSS grafting did not lead to significant modifications of the PCL intrinsic properties.

The only changes in PCL films after pNaSS grafting concerned the surface properties. The relatively low increase of wettability is in good agreement with the low amount of pNaSS determined by the toluidine blue method. Moreover, all the surface analyses demonstrated that the thickness of the pNaSS overlayer is thin. Indeed, the XPS high-resolution C1 s revealed a small decrease in the amount of carboxylate ester species (elements unique to

PCL) and EDX elemental mapping underscored that sulfur atoms do not cover the PCL surface densely. The elemental analyses by EDX and XPS pointed out the low amount of sulfur and sodium (elements unique to pNaSS), as well as small changes in the carbon and oxygen concentrations (elements present in both PCL and pNaSS). Moreover, the difference in sulfur and sodium contents between EDX and XPS analyses is also in good agreement with the small thickness of pNaSS overlayer. Indeed, EDX can be considered as a bulk-sensitive technique which emphasizes the bulk of the material rather than the surface, while XPS is a surface-sensitive technique.

Finally, the stability of the grafted layer under incubation demonstrated that pNaSS was grafted from the PCL films in a stable and covalent manner.

4.3 In vitro assays

Preliminary in vitro tests were carried out to validate the effect of the pNaSS grafting on cell behavior. The results revealed that there were noticeable differences in the cell metabolic activity, the morphology, as well as the adhesion strength of the adherent cells. Indeed, the decrease of cell coverage of the ungrafted PCL film surface could be explained by the removal of cells during the staining process done prior to the fluorescence analysis. This result further demonstrated that cell adhesion strength was improved when pNaSS was grafted from PCL films. Tamada and Ikada [31] reported that fibroblasts had a maximum of adhesion on substrates having a moderate wettability (i.e., water contact angle from 60° to 80°). However with moderate water contact angle before and after pNaSS grafting, the change in wettability is not sufficient to explain the difference in the cell response observed in this study.

The most important surface property modification provided by grafting pNaSS from PCL films is its charge structure. As a matter of fact, the better fibroblast response provided by the grafted surface is assigned to the peculiar surface negative charge provided by the location of the sulfonate group on the aromatic ring of pNaSS [8, 9]. Indeed, the sulfonate groups stimulate cell adhesion and activate cell spreading because the sulfonate groups allow the modulation of the adsorption of adhesive proteins and their folding [32, 33]. Recently, our group demonstrated that only limited protein adsorption from cell culture serum occurs at the surface of ungrafted PCL films whereas pNaSS grafting increased protein adsorption by 75 % [19]. This result well explains the enhancement of fibroblast behavior towards the PCL materials grafted with pNaSS.

Finally, the density of the functional groups also plays important roles for cell adhesion, proliferation, and spreading [9]. Kowalczyńska et al. [33] demonstrated that the rate of cell adhesion is higher with high sulfonated surface, while the rate of spreading is enhanced with low sulfonated surface. As a consequence, the number of spread cells increase when cells are seeded onto surfaces with low sulfonate density and cells possess a larger number of more stable adhesion sites. Therefore, it is possible to conclude that it is not necessary to develop PCL surfaces grafted with high pNaSS density in order to promote the cell response and that a thin layer, as obtained in this study, can provide suitable effects.

5 Conclusion

Sodium styrene sulfonate was successfully grafted onto PCL film surfaces with a homogenous sulfonate distribution. It was demonstrated that the process did not change the intrinsic properties of PCL films and produced a thin overlayer of pNaSS that was found to be reliable and robust, as it was stable during incubation. Despite the small thickness of the pNaSS layer, the bioactivity of PCL was improved as it was found a better adhesion, enhanced spreading and higher metabolic activity of the fibroblast cells which had been seeded onto grafted PCL films. The grafting of pNaSS may effectively modulate the cell response and seems to be a good alternative to develop bioactive polyester-based scaffolds used in tissue engineering applications. For instance, in anterior cruciate ligament reconstruction using connective tissue engineering, recent research has focused on the development of biodegradable structures that could allow a functional graft while enhancing host integration. Based on the results obtained in this study, bioactive and biodegradable prosthetic ligaments based on PCL fibers grafted with pNaSS could be the next generation of synthetic ligaments. The study of pNaSS grafting onto PCL fibers is currently in progress.

Acknowledgments The authors thank the Ministry of National Education, Research and Technology for the MENRT scholarship granted to Stéphane Huot. The XPS experiments were done at NESAC/Bio, which is funded by grant EB-002027 from the US National Institutes of Health. The authors have no conflict of interest to disclose.

References

1. Goddard JM, Hotchkiss JH. Polymer surface modification for the attachment of bioactive compounds. Prog Polym Sci. 2007; 32:698–725.
2. Chan G, Mooney DJ. New materials for tissue engineering: towards greater control over the biological response. Trends Biotechnol. 2008;26:382–92.

3. Tessmar JK, Göpferich AM. Matrices and scaffolds for protein delivery in tissue engineering. Adv Drug Deliver Rev. 2007;59:274–91.
4. Rohman G, Baker SC, Cameron NR, Southgate JJ. Heparin functionalization of porous PLGA scaffolds for controlled, biologically relevant delivery of growth factors for soft tissue engineering. Mater Chem. 2009;19:9265–73.
5. McDonald PF, Lyons JG, Geever LM, Higginbotham CL. *In vitro* degradation and drug release from polymer blends based on poly(DL-lactide), poly(L-lactide-glycolide) and poly(ε-caprolactone). J Mater Sci. 2010;45:1284–92.
6. Eskin SG, Horbett TA, McIntire LV, Mitchell RN, Ratner BD, Schoen FJ, Yee A. Some background concepts. In: Ratner BD, Hoffman AS, Schoen FJ, Lemons JE, editors. Biomaterials science: an introduction to materials in medicine. San Diego: Elsevier Academic Press; 2004. p. 237–91.
7. Li R, Wang H, Wang W, Ye Y. Gamma-ray co-irradiation induced graft polymerization of NVP and SSS onto polypropylene non-woven fabric and its blood compatibility. Radiat Phys Chem. 2013;91:132–7.
8. Kishida A, Iwata H, Tamada Y, Ikada Y. Cell behaviour on polymer surfaces grafted with non-ionic and ionic monomer. Biomaterials. 1991;12:786–92.
9. Lee JH, Lee JW, Khangt G, Lee HB. Interaction of cells on chargeable functional group gradient surfaces. Biomaterials. 1997;18:351–8.
10. Pavon-Djavid G, Gamble LJ, Ciobanu M, Gueguen V, Castner DG, Migonney V. Bioactive PET fibers and fabrics: grafting, chemical characterization and biological assessment. Biomacromolecules. 2007;8:3317–25.
11. Viateau V, Zhou J, Guérard S, Manassero M, Thourot M, Anagnostou F, Mitton D, Brulez B, Migonney V. Ligart: synthetic « bioactive » and « biointegrable » ligament allowing a rapid recovery of patients: chemical grafting, in vitro and in vivo biological evaluation, animal experiments, preclinical study. IRBM. 2011;32:118–22.
12. Oughlis S, Lessim S, Changotade S, Bollotte F, Poirier F, Helary G, Lataillade JJ, Migonney V, Lutomski D. Development of proteomic tools to study protein adsorption on a biomaterial titanium grafted with poly(sodium styrene sulfonate). J Chromatogr B. 2011;879:3681–7.
13. Helary G, Noirclere F, Mayingi J, Migonney V. A new approach to graft bioactive polymer on titanium implants: improvement of MG 63 cell differentiation onto this coating. Acta Biomater. 2009;5:124–33.
14. Oughlis S, Lessim S, Changotade S, Poirier F, Bollotte F, Peltzer J, Felgueiras H, Migonney V, Lataillade JJ, Lutomski D. The osteogenic differentiation improvement of human mesenchymal stem cells on titanium grafted with polyNaSS bioactive polymer. J Biomed Mater Res A. 2013;101:582–9.
15. Zorn G, Baio JE, Weidner T, Migonney V, Castner DG. Characterization of poly(sodium styrene sulfonate) thin films grafted from functionalized titanium surfaces. Langmuir. 2011;27:13104–12.
16. Vaquette C, Viateau V, Guérard S, Anagnostou F, Manassero M, Castner DG, Migonney V. The effect of polystyrene sodium sulfonate grafting on polyethylene terephthalate artificial ligaments on in vitro mineralisation and in vivo bone tissue integration. Biomaterials. 2013;34:7048–63.
17. Nasef MM, Saidi H, Dahlan KZM. Kinetic investigations of graft copolymerization of sodium styrene sulfonate onto electron beam irradiated poly(vinylidene fluoride) films. Radiat Phys Chem. 2011;80:66–75.
18. Huot S, Rohman G, Riffault M, Pinzano A, Grossin L, Migonney V. Increasing the bioactivity of elastomeric poly(ε-caprolactone) scaffolds for use in tissue engineering. Bio-Med Mater Eng. 2013;23:281–8.
19. Djaker N, Brustlein S, Rohman G, Huot S, Lamy de la Chapelle M, Migonney V. Characterization of a synthetic bioactive polymer by nonlinear optical microscopy. Biomed. Opt Express. 2014;5:149–57.
20. Woodruff MA, Hutmacher DW. The return of a forgotten polymer—polycaprolactone in the 21st century. J Prog Polym Sci. 2010;35:1217–56.
21. Wang K, Jesse S, Wang S. Banded spherulitic morphology in blends of poly(propylene fumarate) and poly(ε-caprolactone) and interaction with MC3T3-E1 cells. Macromol Chem Phys. 2012;213:1239–50.
22. Suh H, Hwang Y-S, Lee J-E, Han CD, Park J-C. Behavior of osteoblasts on a type I atelocollagen grafted ozone oxidized poly L-lactic acid membrane. Biomaterials. 2001;22:219–30.
23. Kweon HY, Yoo MK, Park IK, Kim TH, Lee HC, Lee HS, Oh JS, Akaike T, Cho CS. A novel degradable polycaprolactone networks for tissue engineering. Biomaterials. 2003;24:801–8.
24. Baker SC, Rohman G, Southgate J, Cameron NR. The relationship between the mechanical properties and cell behaviour on PLGA and PCL scaffolds for bladder tissue engineering. Biomaterials. 2009;30:1321–8.
25. Yang JC, Jablonsky MJ, Mays JW. NMR and FT-IR studies of sulfonated styrene-based homopolymers and copolymers. Polymer. 2002;43:5125–32.
26. Razumovskii SD, Kefeli AA, Zaikov GE. Degradation of polymers in reactive gases. Eur Polym J. 1971;7:275–85.
27. Kulik EA, Ivanchenko M, Kato K, Sano S, Ikada Y. Peroxide generation and decomposition on polymer surface. J Polym Sci A: Polym Chem. 1995;33:323–30.
28. Chen J, Nho Y-C, Park J-S. Grafting polymerization of acrylic acid onto preirradiated polypropylene fabric. Radiat Phys Chem. 1998;52:201–6.
29. Ohrlander M, Wirsen A, Albertsson A-C. The grafting of acrylamide onto poly(ε-caprolactone) and poly(1,5-dioxepan-2-one) using electron beam preirradiation. I. Influence of dose and Mohr's salt for the grafting onto poly(ε-caprolactone). J Polym Sci A: Polym Chem. 1999;37:1643–9.
30. Natu MV, de Sousa HC, Gil MH. Influence of polymer processing technique on long term degradation of poly(ε-caprolactone) constructs. Polym Deg Stab. 2013;98:44–51.
31. Tamada Y, Ikada Y. Effect of preadsorbed proteins on cell adhesion to polymer surfaces. J Colloid Interface Sci. 1993;155:334–9.
32. Kowalczyńska HM, Nowak-Wyrzykowska M, Dobkowski J, Kołos R, Kamiński J, Makowska-Cynka A, Marciniak E. Adsorption characteristics of human plasma fibronectin in relationship to cell adhesion. J Biomed Mater Res. 2002;61:260–9.
33. Kowalczyńska HM, Nowak-Wyrzykowska M. Modulation of adhesion, spreading and cytoskeleton organization of 3T3 fibroblasts by sulfonic groups present on polymer surfaces. Cell Biol Int. 2003;27:101–14.